

# Supplemental Tables and Figures

## MOL #96883

### **Synthesis and Evaluation of a Novel Deguelin Derivative, L80, which Disrupts ATP Binding to the C-terminal Domain of Heat Shock Protein 90**

Su-Chan Lee, Hye-Young Min, Hoon Choi, Ho Shin Kim, Kyong-Cheol Kim, So-Jung Park, Myung A Sung, Ji Hae Seo, Hyun-Ju Park, Young-Ger Suh, Kyu-Won Kim, Jeewoo Lee, Ho-Young Lee

College of Pharmacy and Research Institute of Pharmaceutical Sciences, Seoul National University, Seoul 151-742, Republic of Korea ( S.C.L., H.Y.M., H.C., H.S.K., K.C.K., M.A.S., J.H.S., Y.G.S., K.W.K., J.L., H.Y.L.)  
School of Pharmacy, Sungkyunkwan University, Suwon 440-746, Korea (S.J.P., H.J.P.)

**Table S1.** BBB permeability of deguelin, L80, progesteron, and theophylline as determined by the Parallel Artificial Membrane Permeability assay.

<b>Compound</b>	<b>-log <math>P_e</math>*</b>	<b>CNS+/- prediction</b>
<b>Degueline</b>	4.78±0.20	+
<b>L80</b>	4.82±0.25	+
Progesteron <sup>†</sup>	4.62±0.11	+
Theophylline <sup>†</sup>	6.77±0.30	-

\*Average  $-\log P_e$  values were calculated by the PAMPA Explorer software v. 3.5.

<sup>†</sup> Progesteron, and theophylline were selected for comparison based on their known CNS activity

**Table S2.** Histology and genetic background of used cell lines

	<b>EGFR</b>	<b>K-Ras</b>	<b>p53</b>	<b>PTEN</b>	<b>PI3KCA</b>	<b>LKB1</b>	<b>B-Raf</b>
<b>A549</b>	WT	Mut	WT	WT	WT	Mut	WT
<b>H226B</b>	WT	WT	WT	U	WT	WT	WT
<b>H1299</b>	WT	WT	Nu	Nu	WT	WT	WT
<b>H460</b>	WT	Mut	WT	WT	Mut	Mut	WT

\* WT: wild type Mut: mutant type Nu: null U: unknown

## Supplemental Figure Legends

**Figure S1. Toxicity of L80 compared to deguelin** (A) Blood-Brain-Barrier permeability assay was conducted by using the PAMPA Explorer kit (pION Inc.) Progesterone, and theophylline were used as positive, and negative control. (Pro: progesterone, Theo: theophylline, Deg: deguelin) (B-D) Mouse hippocampal cell (HT-22 cell), Human umbilical vein endothelial (HUVEC), retinal pigment epithelial (RPE), and normal immortalized lung epithelial cells (HBEC and BEAS-2B) were treated with increasing concentrations of L80 or deguelin for 3 days. Values represent mean  $\pm$  SD of experiments conducted in triplicate. \* $p < 0.05$ , \*\* $p < 0.01$ , and \*\*\* $p < 0.001$  by one-way analysis of variance (ANOVA) or Student's t-test compared with control group.

**Figure S2. Inhibitory effects of L80 on the proliferation and colony formation of human lung cancer cells.** (A) H1299, A549, H460, and H226B cells; paclitaxel-resistant lung cancer cells (H460/R and H226B/R); and were treated with increasing concentrations of L80 or deguelin for 3 days. Cell viability was determined by the MTT assay. (B) H1299, A549, H460, H460/R, H226B, and H226B/R cells were seeded onto 6-well plates at a density of 300 cells/well and then treated with L80 (0, 0.1, 1, and 10  $\mu$ M). After two weeks, colonies were stained with crystal violet and counted. (C) The anchorage-independent growth of cells treated with increasing concentrations of L80 was determined by soft agar colony formation assay. All values represent mean  $\pm$  SD of experiments conducted in triplicate. \* $p < 0.05$ , \*\* $p < 0.01$ , and \*\*\* $p < 0.001$  by one-way analysis of variance (ANOVA) compared with control group.

**Figure S3. Induction of apoptosis by treatment with L80.** (A) Cells were treated with L80 for 24 h. The distribution of cells in each phase of the cell cycle was analyzed by flow cytometry.

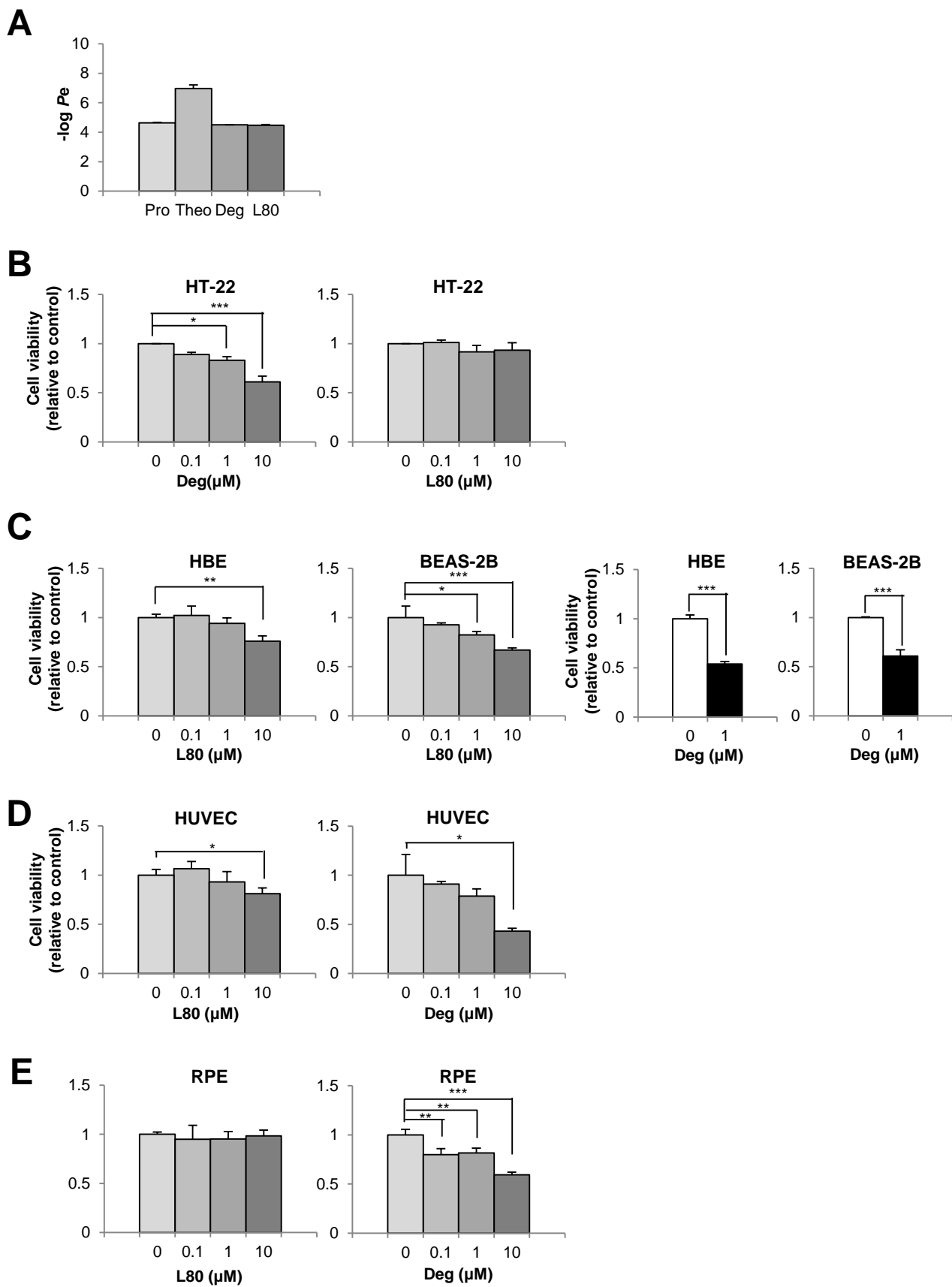
**Figure S4. L80 exerts its antiangiogenic potential through inhibiting the stability and transcriptional activity of HIF-1 $\alpha$ .** (A) The HIF-1 $\alpha$  expression level in the indicated NSCLC cells were treated with increasing concentrations of L80 under hypoxia condition was analyzed by Western blot analysis. (B) The indicated NSCLC cells were co-transfected with pGL3-basic or pGL3-HRE-Luc and pRL-TK-Luc. After treatment with L80 under hypoxia condition, luciferase activity was monitored as described in the Materials and Methods section. Values represent mean  $\pm$  SD of experiments conducted in triplicate. \* $p < 0.05$  by Student's t-test compared with control group. (C, D) The indicated NSCLC cells treated with increasing concentrations of L80 (C) or H1299 treated with 1  $\mu$ M of deguelin or L80 (D) were subjected to RT-PCR for the mRNA expression of VEGF and IGF2. (E) HUVECs were treated with CM obtained from H1299 cells treated with increasing concentrations of L80 and incubated under hypoxic conditions. The morphological changes of HUVECs were imaged and scored. Values represent mean  $\pm$  SD of experiments conducted in triplicate. \* $p < 0.05$ , \*\*\* $p < 0.001$  by one-way analysis of variance (ANOVA) compared with control group (0 $\mu$ M of L80).

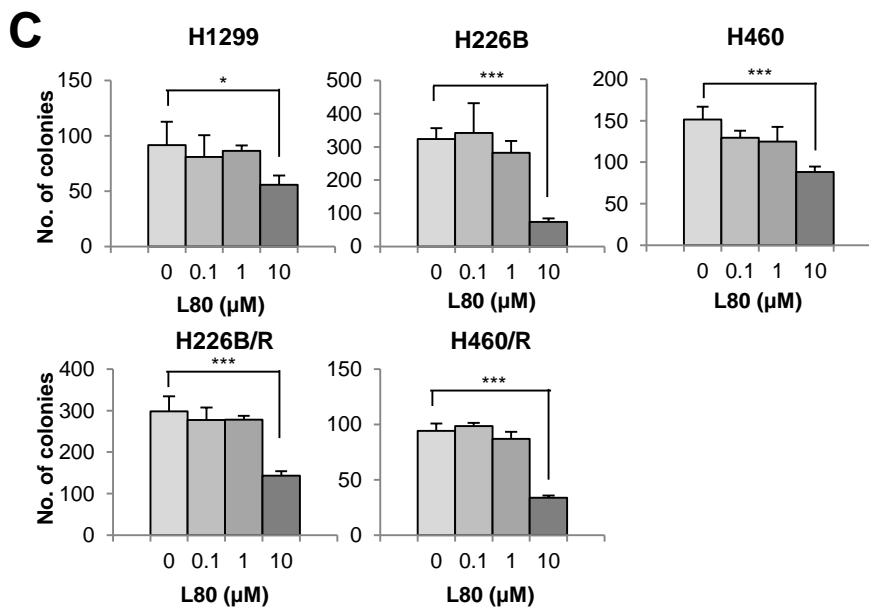
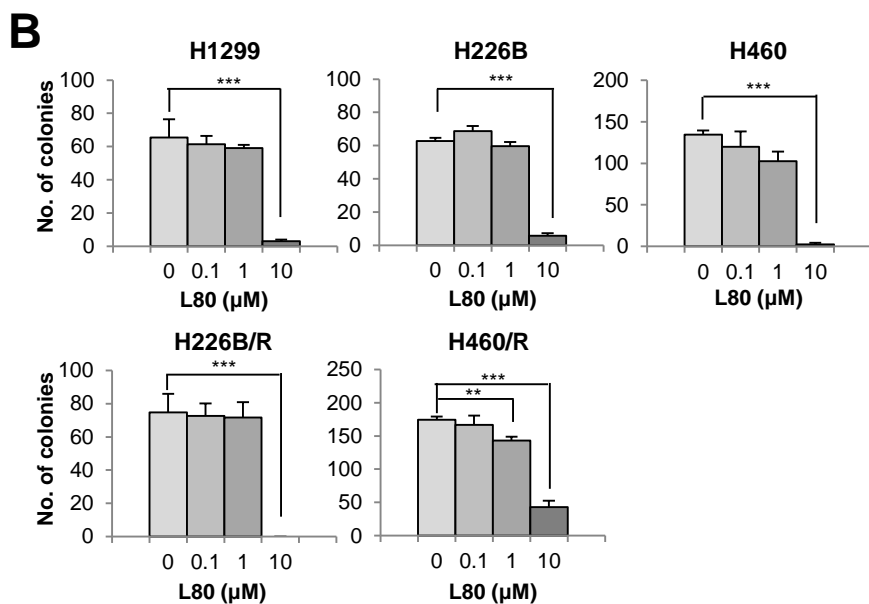
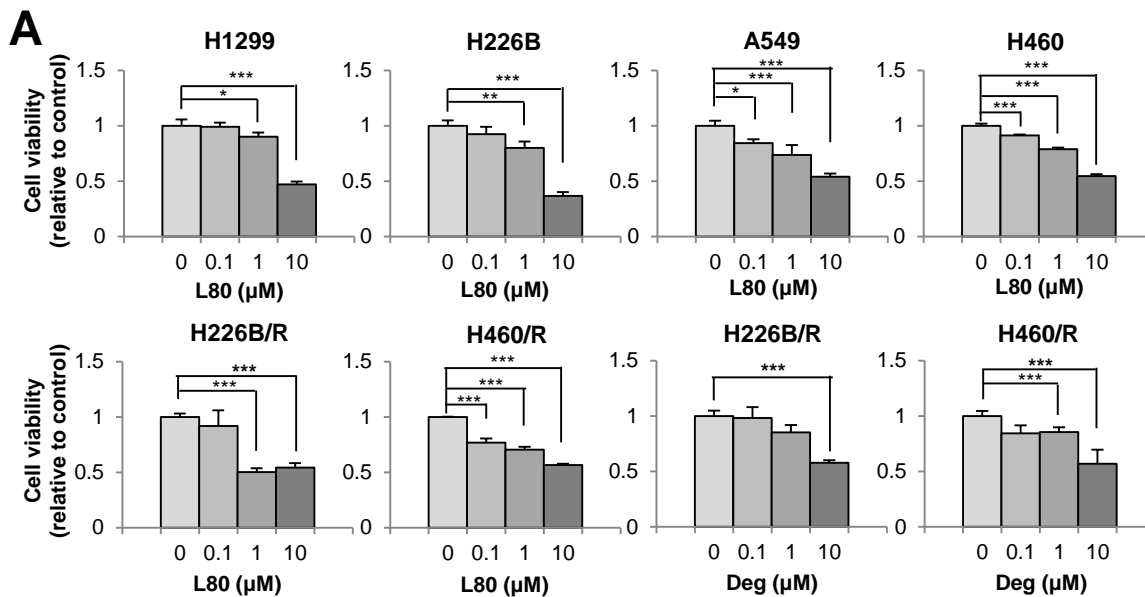
**Figure S5. Inhibition of migration and invasion of lung cancer by treatment with L80.** H1299, H226B, and H226B/R cells were seeded onto 96-well plates and incubated for 12h to evaluate proliferation effects by MTT assay (A). These cells also were seeded onto Transwells coated with either gelatin only (B) or gelatin and matrigel (C). After incubation for 18-19h, the migratory or invaded cells on the bottom of the membrane were stained and counted. All values represent mean  $\pm$  SD of experiments conducted in triplicate. \* $p < 0.05$ , \*\* $p < 0.01$ , and \*\*\* $p < 0.001$  by Student's  $t$ -test compared with control group.

**Figure S6. The effect of L80 on body weight in a tumor xenograft model.** H1299 cells were inoculated into the right flank of NOD/SCID mice. Mice harboring H1299 xenograft tumors were treated with vehicle or L80 for 3 weeks. The body weight were monitored on 1day, and 20days. Body weight was analyzed by one-way analysis of variance (ANOVA) compared with control group (0mg/kg).

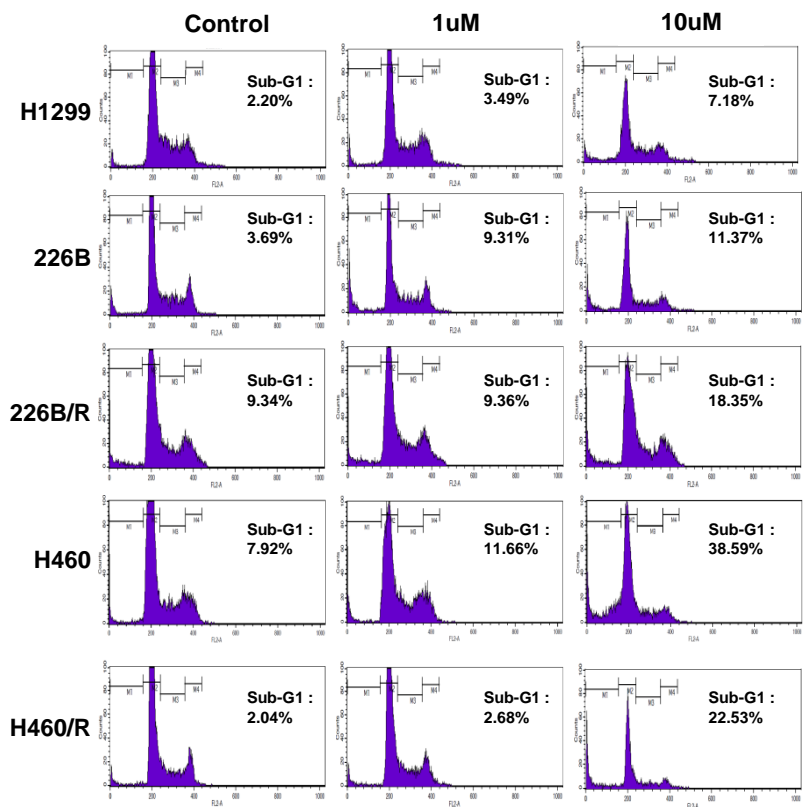
**Figure S7. Downregulation of Hsp90 function by treatment with L80.** (A) H1299 cells were treated with L80 under hypoxic conditions. Total cell lysates were prepared and immunoprecipitated with anti-HIF-1 $\alpha$  antibodies. The interaction between HIF-1 $\alpha$  and Hsp90 was analyzed by Western blot analysis. (B) H1299 lysates interacted with histidine-tagged recombinant HIF-1 $\alpha$  in the presence or absence of L80. After pull-down with Ni-NTA agarose beads, the amount of Hsp90 bound to the recombinant HIF-1 $\alpha$  was determined by Western blot analysis. (C) The expression levels of ErbB2 and Akt in the initiated NSCLC cells treated with increasing concentrations of L80 were analyzed by Western blot analysis. (D) Recombinant Hsp90 proteins containing the FL protein or the NM, M, and C domains interacted with ATP-agarose in the presence or absence of L80. The protein level bound to the ATP-agarose beads was determined by Western blot analysis.

**Figure S8. Full blots of cleaved parp in NSCLC cells.** H1299, H226B, H460, H226B/R, and H460/R cells were seeded and treated with 0, 1, and 10  $\mu$ M L80 for 24 h. Cell lysates were obtained by RIPA buffer and determined by Western blot analysis.



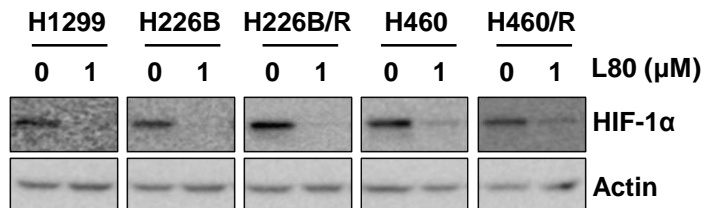


**A**

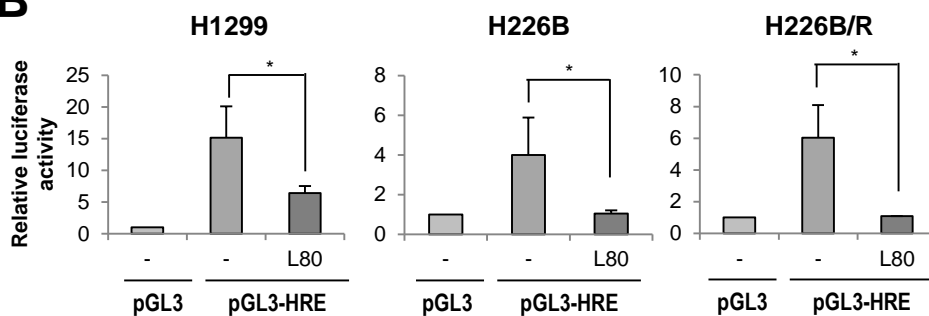




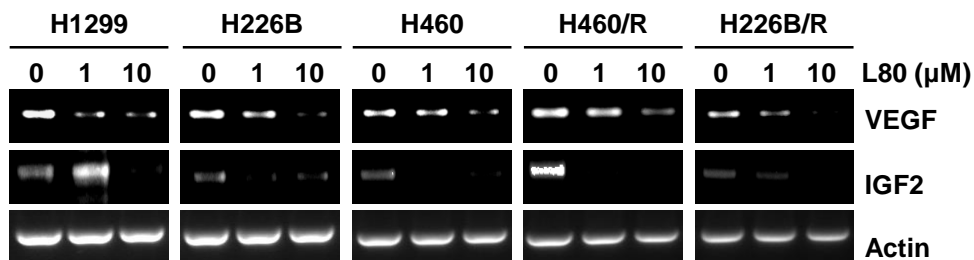
**A**



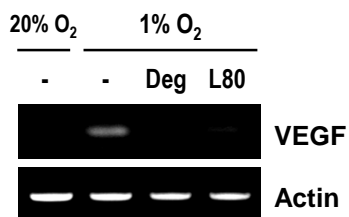
**B**



**C**



**D**



**E**

